



Original

Calcium and integrin binding protein 1 (CIB1) induces myocardial fibrosis in myocardial infarction via regulating the PI3K/Akt pathway

Guangquan HU^{1,2}, Xiaojie DING³, Feng GAO² and Jiehua LI¹

¹Department of Geriatric Cardiology, The First Affiliated Hospital of Anhui Medical University, No. 218, Jixi Road, Hefei 230022, P.R. China

²Department of Internal Medicine-Cardiovascular, The Second Hospital of Anhui Medical University, No. 678, Furong Road, Economic Development Zone, Hefei 230601, P.R. China

³Department of Endocrinology, Anhui No.2 Provincial People's Hospital, No. 1868, North Second Ring Dangshan Road, Yaohai District, Hefei 230041, P.R. China

Abstract: Myocardial infarction (MI) is a severe coronary artery disease resulted from substantial and sustained ischemia. Abnormal upregulation of calcium and integrin binding protein 1 (CIB1) has been found in several cardiovascular diseases. In this study, we established a mouse model of MI by permanent ligation of the left anterior descending coronary artery. CIB1 was upregulated in the heart of MI mice. Notably, CIB1 knockdown by intramuscular injection of lentivirus-mediated short hairpin RNA (shRNA) targeting *Cib1* improved cardiac function and attenuated myocardial hypertrophy and infarct area in MI mice. MI-induced upregulation of α -SMA, vimentin, Collagen I, and Collagen III, which resulted in collagen production and myocardial fibrosis, were regressed by CIB1 silencing. *In vitro*, cardiac fibroblasts (CFs) isolated from mice were subjected to angiotensin II (Ang II) treatment. Inhibition of CIB1 downregulated the expression of α -SMA, vimentin, Collagen I, and Collagen III in Ang II-treated CFs. Moreover, CIB1 knockdown inhibited Ang II-induced phosphorylation of PI3K-p85 and Akt in CFs. The effect of CIB1 knockdown on Ang II-induced cellular injury was comparable to that of LY294002, a specific inhibitor of the PI3K/Akt pathway. We demonstrated that MI-induced cardiac hypertrophy, myocardial fibrosis, and cardiac dysfunction might be attributed to the upregulation of CIB1 in MI mice. Downregulation of CIB1 alleviated myocardial fibrosis and cardiac dysfunction by decreasing the expression of α -SMA, vimentin, Collagen I, and Collagen III via inhibiting the PI3K/Akt pathway. Therefore, CIB1 may be a potential target for MI treatment.

Key words: calcium and integrin binding protein 1 (CIB1), collagen production, myocardial fibrosis, myocardial infarction, PI3K/Akt pathway

Introduction

Myocardial infarction (MI), a leading cause of death among all cardiovascular diseases, is characterized by cardiomyocyte death resulting from substantial and sustained ischemia due to imbalances between myocardial oxygen supply and demand [1, 2]. Acute myocardial infarction is the most severe manifestation of coronary artery disease with high morbidity and mortality. It can

consequently result in the development of chronic heart failure and has a significant impact on global health, affecting more than 7 million people worldwide each year [3, 4]. Although early treatment with reperfusion and pharmacotherapy has contributed to a conspicuous decline in mortality after acute MI, current therapies for heart failure after MI is limited and non-curative, and the efforts remain to be urgently needed to minimize the mortality and economic cost in the disease treatment [5, 6].

(Received 15 April 2021 / Accepted 1 July 2021 / Published online in J-STAGE 4 August 2021)

Corresponding author: J. Li. email: aydlilaoshi@163.com



This is an open-access article distributed under the terms of the Creative Commons Attribution Non-Commercial No Derivatives (by-nc-nd) License <<http://creativecommons.org/licenses/by-nc-nd/4.0/>>.

©2022 Japanese Association for Laboratory Animal Science

Calcium and integrin binding protein 1 (CIB1), which was first discovered as a binding partner of the α IIb integrin cytoplasmic domain in platelets, can bind to different proteins in diverse cells, exhibiting a broad functional versatility in multiple cellular processes, such as adhesion, migration, and Ca^{2+} signaling to cell survival and proliferation. Increasing evidence also indicates a novel role of CIB1 in cancer and cardiovascular disease [7, 8]. CIB1 mediates tumor growth and angiogenesis by repressing tumor cell apoptosis and promoting tumor cell proliferation and migration [9–11]. CIB1 is widely expressed in multiple tissues or organs of humans and mice, particularly highly expressed in the heart [12, 13]. The level of urine CIB1 in patients with both acute and chronic ischemic heart failure is significantly higher than that in healthy individuals [14]. Besides, it also is up-regulated both in the right atrial myocardium of patients with atrial fibrillation and in the peripheral blood mononuclear cells of patients with the acute coronary syndrome [15, 16]. Moreover, CIB1 expression is strongly induced in cardiomyocytes by hypertrophy. The contribution of CIB1 to transverse aortic constriction (TAC)-induced cardiac hypertrophy model has been investigated [17]. CIB1 overexpression aggravates cardiac hypertrophy in response to pressure overload, while CIB1 deficiency inhibits pathological cardiac growth. Besides, CIB1 deletion also reduced myocardial fibrosis and cardiac dysfunction in the mice after pressure overload [17]. However, the role of CIB1 in MI and the underlying mechanism have not been explored yet. In our research, MI model was established by left anterior descending coronary artery (LAD) ligation [18, 19]. TAC-induced cardiac hypertrophy and LAD ligation-induced MI are both models of heart failure, but they have different pathogenesis mechanisms. TAC triggers the exposure of the heart to high pressure and cardiac hypertrophy, while LAD induces ischemic heart failure [20, 21]. The findings above suggest a vital role of CIB1 in heart diseases.

An increasing number of studies report that the phosphatidylinositol 3-kinase (PI3K)/protein kinase B (Akt) pathway is involved in cardiac fibrosis [22, 23]. PI3K is a protein consisting of a regulatory subunit p85 and a catalytic subunit p110. Activation of the p85 subunit leads to activation of p110, inducing the phosphorylation and activation of Akt [24]. In this study, to investigate CIB1 role in MI-induced myocardial fibrosis and whether CIB1 functions in this process *via* regulating the PI3K/Akt pathway, we established the MI model *in vivo* *via* LAD ligation and assessed angiotensin II (Ang II)-inducing fibrosis *in vitro* using cardiac fibroblasts. Cardiac fibrosis is a common feature after MI. By experi-

ments *in vivo* and *in vitro*, we demonstrate that CIB1 knockdown plays a protective role in MI *via* inhibiting myocardial fibrosis, which may provide new insight into MI progression and therapy.

Materials and Methods

Animal model

Permanent ligation of the left anterior descending coronary artery (LAD) was performed on 8-week-old C57BL/6 male mice purchased from Liaoning Changsheng Biotechnology Co., Ltd. (Benxi, China) to induce myocardial infarction (MI), as previously described [25, 26]. Briefly, mice were anesthetized with an intraperitoneal injection of 50 mg/kg sodium pentobarbital (Xiya reagent, Linyi, China). The trachea was exposed after a median neck incision and then split horizontally for 2–3 mm. A plastic cannula was intubated into the trachea and connected to a rodent ventilator. Next, a left thoracotomy was carried out between the third and the fourth intercostal rib space to expose the heart. LAD was ligated permanently using a 7–0 silk suture, and then the chest was then closed. The same operation was performed on sham-operated mice without LAD ligation. During the whole process, the mice's body temperature was maintained at about 37°C. The animal experiments were approved by the ethics committee of the First Affiliated Hospital of Anhui Medical University (No. LLSC20201117).

To detect CIB1 expression, the sham-operated and MI mice were anesthetized by an overdose of sodium pentobarbital (200 mg/kg) for euthanasia at 1 and 4 weeks post-MI, and the heart tissues were separated. In addition, some heart tissues were frozen in liquid nitrogen and store at -70°C , and some were fixed with 4% paraformaldehyde (Aladdin, Shanghai, China).

To investigate CIB1 function in MI, the sham-operated mice were subjected to multipoint intramyocardial injection of equivalent PBS (Wanleibio, Shenyang, China) without LAD ligation. Multipoint intramyocardial injection (5 points, 2 μl /point) of PBS, 5×10^6 transducing units of *Cib1* RNA-interfering lentivirus (LV-sh*Cib1*), or its negative control lentiviral (LV-shNC) was performed respectively before LAD ligation during the MI surgery (Fig. 1). Six mice were used for analysis in each group. Four weeks later, the mice were euthanized, and some heart tissues were used to separate the left ventricle and calculated each ratio of left ventricle weight to the bodyweight of the mouse. The other heart tissues were used to measure the infarct area with 2, 3, 5-triphenyltetrazoliumchloride (TTC) staining and frozen in liquid nitrogen before stored at -70°C .

Echocardiography (Echo)

Four weeks after MI modeling, the left ventricular function of the mice, including left ventricular end-diastolic dimension (LEVDd), left ventricular end-systolic dimension (LVESd), fractional shortening (FS,%), and ejection fraction (EF,%), was assessed with echocardiography.

Quantitative real-time PCR

The total RNA isolation reagent TRIpure (Biotek, Beijing, China) was used to extract RNA in tissues or cells. Then RNA was reverse-transcribed by Super M-MLV reverse transcriptase (Biotek), and cDNA was amplified with 2×Taq PCR MasterMix (Solarbio, Beijing, China) and detected on Exicycler™ 96 Real-time PCR System (Bioneer Corporation, Daejeon, Korea). The primers were synthesized by Genscript Biotechnology Co., Ltd. (Nanjing, China) and listed in Table 1.

Western blot analysis

The proteins isolated from tissues or cells were quantified using BCA Kit (Beyotime, Shanghai, China). Equal amounts of proteins were separated *via* SDS-PAGE and transferred onto polyvinylidene difluoride (PVDF; Thermo Scientific, Pittsburgh, PA, USA) membranes. The membrane was blocked with 5% bovine serum al-

bumin (BSA; Biosharp, Hefei, China) and incubated with the anti-CIB1 antibody (Cat.No.A4430; dilution, 1:1,000; Abclonal, Wuhan, China), anti-PI3K-p85 antibody (Cat. No. AF6241; dilution, 1:1,000; Affinity, Cincinnati, OH, USA), anti-p-PI3K-p85 antibody (Cat.No. AF3242; dilution, 1:1,000; Affinity), anti-Akt antibody (Cat.No. AF6261; dilution 1:1,000; Affinity), anti-p-Akt antibody (Cat.No. AF0016; dilution 1:1,000; Affinity), anti- α -SMA antibody (Cat.No. AF1032; dilution 1:1,000; Affinity), and anti-Collagen I antibody (Cat.No. AF7001; dilution 1:1,000; Affinity) at 4°C overnight, followed by the secondary antibody horseradish peroxidase-linked IgG (Cat.No. SA00001-2; dilution, 1:10,000; Proteintech Group, Rosemont, IL, USA) for 40 min at 37°C. All protein bands became visible using enhanced chemiluminescence (ECL; Seven-sea pharmtech, Shanghai, China), and the density of each band was quantified.

Measurement of myocardial infarct size

Infarct size was determined by TTC staining. After euthanasia, the left ventricular was excised from the heart and frozen at -20°C immediately for 3 h. Then they were cut into five 1-mm-thick transverse slices parallel to the atrioventricular groove. Five sections in each group were incubated with 2% TTC (Solarbio) solution in the dark at 37°C for 30 min. The ratio of infarct area (pale) to LV area was calculated using Image-Pro Plus software 6.0 (Media Cybernetics, Inc., Bethesda, MD, USA).

Histological analysis

Cardiomyocyte short axis diameter was measured on the images from hematoxylin (Solarbio) and eosin (Sangon, Shanghai, China) stained heart tissue sections. Short axis diameter was measured in three different random areas at 600× magnification. Masson's trichrome staining was performed to evaluate the severity of myocardial fibrosis. The tissue slides embedded in paraffin were stained with hematoxylin (Solarbio) solution, ponceau (Sinopharm, Beijing, China), and acid fuchsin (Sinopharm) solution, and toluidine blue (Sinopharm) in turn. The images were captured at 200× magnification under a fluorescence microscope (BX53, Olympus, Tokyo, Japan). The collagen fibers were stained blue, and the cell

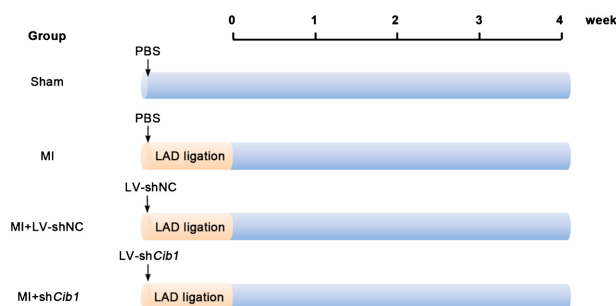


Fig. 1. The diagram of treatments for CIB1 function analysis in the myocardial infarction (MI). MI model was established on 8-week-old male C57BL/6 mice with permanent ligation of the left anterior descending coronary artery (LAD). Multipoint intramyocardial injection of *Cib1* RNA-interfering lentivirus (LV-sh*Cib1*) was performed before LAD ligation for CIB1 knockdown. PBS: phosphate buffer saline. LV-shNC: negative control lentivirus.

Table 1. The primers used for real-time PCR

Gene	Forward (5'-3')	Reverse (5'-3')
<i>Cib1</i>	GATGACGATGGAACCCTG	ATGCTGGAACCTCGGAAAG
<i>Vim</i>	TTGAACGAAAAGTGGAAATC	AGGTCAGGCTTGGAAACG
<i>Colla1</i>	AAGAACCCTGCCCGCACATG	GAATCCATCGGTCATGCTCT
<i>Col3a1</i>	GCCACAGCCTTCTACACCT	GATAGCCACCCATTCCTCCC
<i>β-actin</i>	CTGTGCCCATCTACGAGGGCTAT	TTTGATGTCACGCACGATTTC

cytoplasm was stained red. For quantification, the ratio of fibrosis area to the entire area was measured using Image-Pro Plus software 6.0 (Media Cybernetics, Inc.).

In immunohistochemical staining, the heart tissues fixed with 4% paraformaldehyde were embedded in paraffin and dissected into 5- μ m sections. After subjected to deparaffinization, rehydration, and antigen retrieval, the slides were incubated with 3% H₂O₂ (Sinopharm) solution for 15 min. Then the slides were blocked with goat serum (Solarbio) and incubated with anti-CIB1 antibody (Cat.No. A4430; dilution, 1:200; Abclonal) at 4°C overnight. After the tissues were washed, they were probed with horseradish peroxidase-labeled goat anti-rabbit IgG (Cat.No. #31460; dilution, 1:500; ThermoFisher Scientific, Pittsburgh, PA, USA) at 37°C for 60 min. Subsequently, the tissue slides were stained with 3, 3'-diaminobenzidine (DAB; Solarbio) followed by counterstaining with hematoxylin (Solarbio) and dehydration with xylene. Representative photographs of immunohistochemistry were captured under a microscope (BX53, Olympus). Integrated option density summation (IOD SUM) of CIB1-positive cells and area were measured by Image-Pro Plus software 6.0 (Media Cybernetics, Inc.). The mean density was used to represent CIB1 expression.

Isolation and culture of murine primary cardiac fibroblasts

After euthanasia with sodium pentobarbital (200 mg/kg), hearts were separated from 3-day-old C57BL/6 mice and finely minced into small pieces under sterile conditions. The pieces were digested with 0.025 mg/ml of Liberase TM solution containing collagenase I and II (Roche, Basel, Switzerland) and DNase (40 μ g/ml; Aladdin) in serum-free Dulbecco's modified Eagle's (DMEM) medium (Gibco, Grand Island, NY, USA) at 37°C for 45 min. Then cell suspensions were filtered through a 70- μ m aperture sieve and centrifuged at 50 g for 2 min. The supernatants were filtered through a 40- μ m aperture sieve and centrifuged at 450 g for 4 min. Cells were gathered at the bottom of the tube, resuspended in DMEM medium containing 10% fetal bovine serum (FBS; Biological Industries, Kibbutz Beit-Haemek, Israel), and then cultured at 37°C in 5% CO₂. Fibroblast specific protein 1 (FSP1) immunofluorescence staining was performed to identify the cardiac fibroblasts.

Immunofluorescence (IF) staining

The sections of heart tissues embedded in paraffin were put in citrate solution at a high temperature for antigen retrieval and blocked with goat serum (Solarbio) in a wet box at room temperature for 15 min. Then the

sections were incubated with anti- α -SMA antibody (Cat. No. AF1032; dilution, 1:200; Affinity) or anti-FSP1 antibody (Cat.No. A19109; dilution, 1:200; Abclonal) at 4°C overnight followed by a 60-min incubation with the Cy3-labeled goat anti-rabbit IgG (Cat.No. A0516; dilution, 1:200; Beyotime) in the dark at room temperature. Finally, the cells were counterstained with 4',6-diamidino-2-phenylindole (DAPI; Beyotime), and fluorescence quenching agent resistance (Solarbio) was added. To detect α -SMA or FSP1 expression in the CFs, the cell slides were fixed with paraformaldehyde and subjected to 0.1% Triton X-100 (Beyotime). The following processes were the same with heart tissues. The images were captured at 400 \times magnification under a fluorescence microscope (BX53, Olympus). IOD SUM of α -SMA and area were measured by Image-Pro Plus software 6.0 (Media Cybernetics, Inc.). The mean density was used to quantify the protein expression.

Cell model

The CFs were infected with *Cib1* RNA-interfering lentivirus or NC lentivirus in the culture medium. Forty-eight hours later, 0.1 μ M angiotensin II (Ang II; Aladdin) was added to the medium. The cells were cultured for another 24 h and then were collected for detection. To confirm the effects of CIB1 on the PI3K/Akt pathway, LY294002 (MedChemExpress, Monmouth Junction, NJ, USA), a specific PI3K/Akt pathway inhibitor, was added to treat the CFs before Ang II treatment. There were three replicates in each group.

Statistical analysis

The data were represented as mean \pm SD and subjected to multiple comparisons with ANOVA. *P* value less than 0.05 suggested that the difference was statistically significant. GraphPad Prism 7.0 software (GraphPad Software Inc., La Jolla, CA, USA) was used for analysis and histograms.

Results

The expression of CIB1 is upregulated in the heart of MI mice

The mRNA and protein expression of CIB1 was measured at 1 and 4 weeks post-MI. The immunohistochemistry staining of CIB1 in the penumbra of the ischemic heart showed an enhanced CIB1 expression in cardiomyocytes of MI mice compared with sham-operated mice both at 1 and 4 weeks post-MI (Figs. 2A and B). Likewise, the mRNA of *Cib1* detected with real-time PCR also exhibited a higher level in the penumbra of the ischemic heart of MI mice than in sham-operated mice

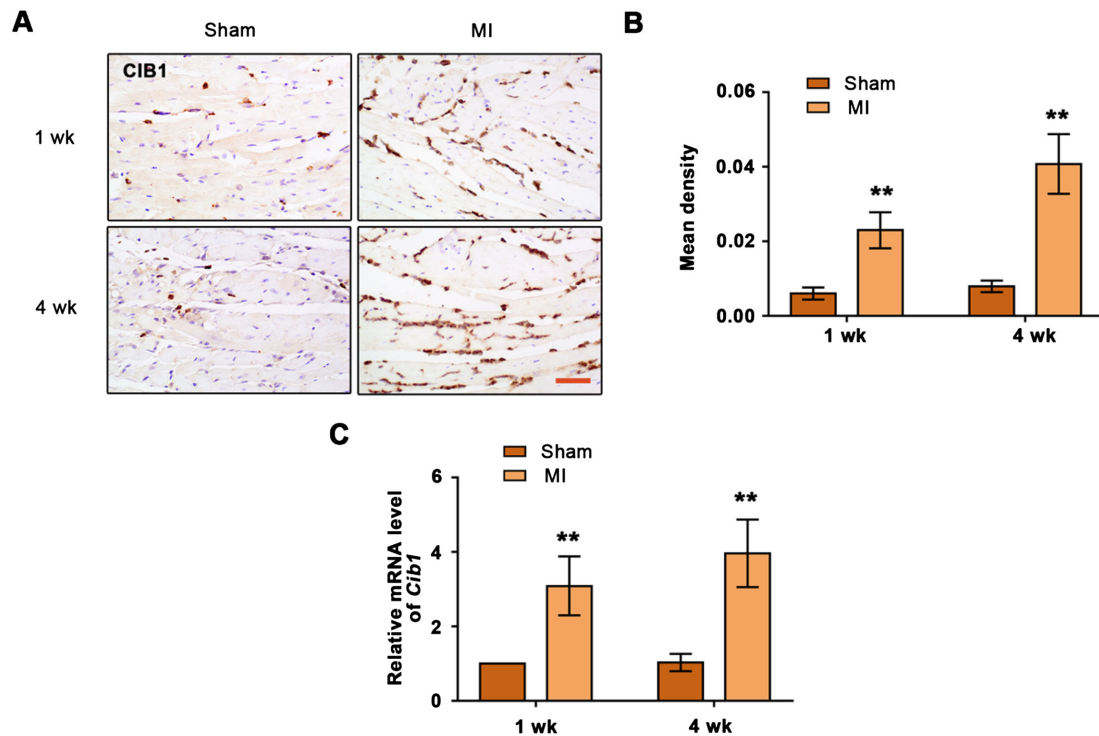


Fig. 2. CIB1 expression is upregulated in the heart of MI mice. A. The expression and location of CIB1 in the penumbra of ischemic heart at 1 and 4 weeks post-MI detected with immunohistochemistry. Magnification: 400 \times . Scale bar=50 μ m. B. Quantification of CIB1 expression in immunohistochemistry. C. The mRNA level of *Cib1* in the penumbra of ischemic heart at 1 and 4 weeks post-MI. Data are expressed as the mean \pm SD (n=6/group). ** P <0.01 vs. Sham group.

(Fig. 2C), suggesting that MI strongly induces CIB1 expression in the heart.

CIB1 silencing relieves MI-induced myocardial damage and improves cardiac dysfunction

The decreased protein level of CIB1 in the penumbra of the ischemic heart of MI mice indicated that the infection of *Cib1* RNA-interfering lentivirus knocked down CIB1 in mice successfully (Figs. 3A and B). To investigate the effects of downregulation of CIB1 on cardiac function, the cardiac function indexes such as LVEDd, LVEDs, FS, and EF were measured with Echo. MI significantly markedly increased LVEDd and LVESd but lowered FS and EF when compared with sham group. While the silencing of CIB1 mediated by LV-sh*Cib1* reduced LVEDd and LVESd but elevated FS and EF to levels close to those in sham group (Table 2), suggesting that CIB1 silencing improved MI-induced cardiac dysfunction in mice. Besides, the infarction area stained by TTC showed that the knockdown of CIB1 reduced the infarction area of the heart, which was dramatically enlarged by MI (Figs. 3C and D). Moreover, the left ventricle-to-body weight ratio (LV/BW) was calculated in MI mice. MI notably increased the value of LV/BW compared with sham group while the ratio was regressed

because of the downregulation of CIB1 in MI mice (Fig. 3E). Furthermore, the mean of cardiomyocyte short axis diameter, which was increased by MI, was reduced in the heart tissues when CIB1 was knocked down (Fig. 3F). Therefore, the results above indicate that CIB1 silencing relieves MI-induced myocardial damage, including infarction and cardiac hypertrophy, and improves cardiac dysfunction.

CIB1 knockdown alleviates myocardial fibrosis caused by MI in mice

The fibrosis in the penumbra of ischemic heart was stained by Masson's trichrome staining. Less collagen deposition in the penumbra of ischemic heart was observed in MI mice infected with LV-sh*Cib1*, and quantitative analysis revealed that the percent of myocardial fibrosis area was reduced in MI mice after CIB1 knockdown (Figs. 4A and B). The expression of α -SMA is considered an indicator of differentiated myofibroblasts. Besides, FSP1 is also an indicator of fibroblast/myofibroblast phenotypes. Immunofluorescence staining showed that the numbers of FSP1- and α -SMA-positive cells were increased by MI while regressed by CIB1 silencing (Fig. 4C). This was supported by the quantification of α -SMA immunofluorescence staining (Fig. 4D),

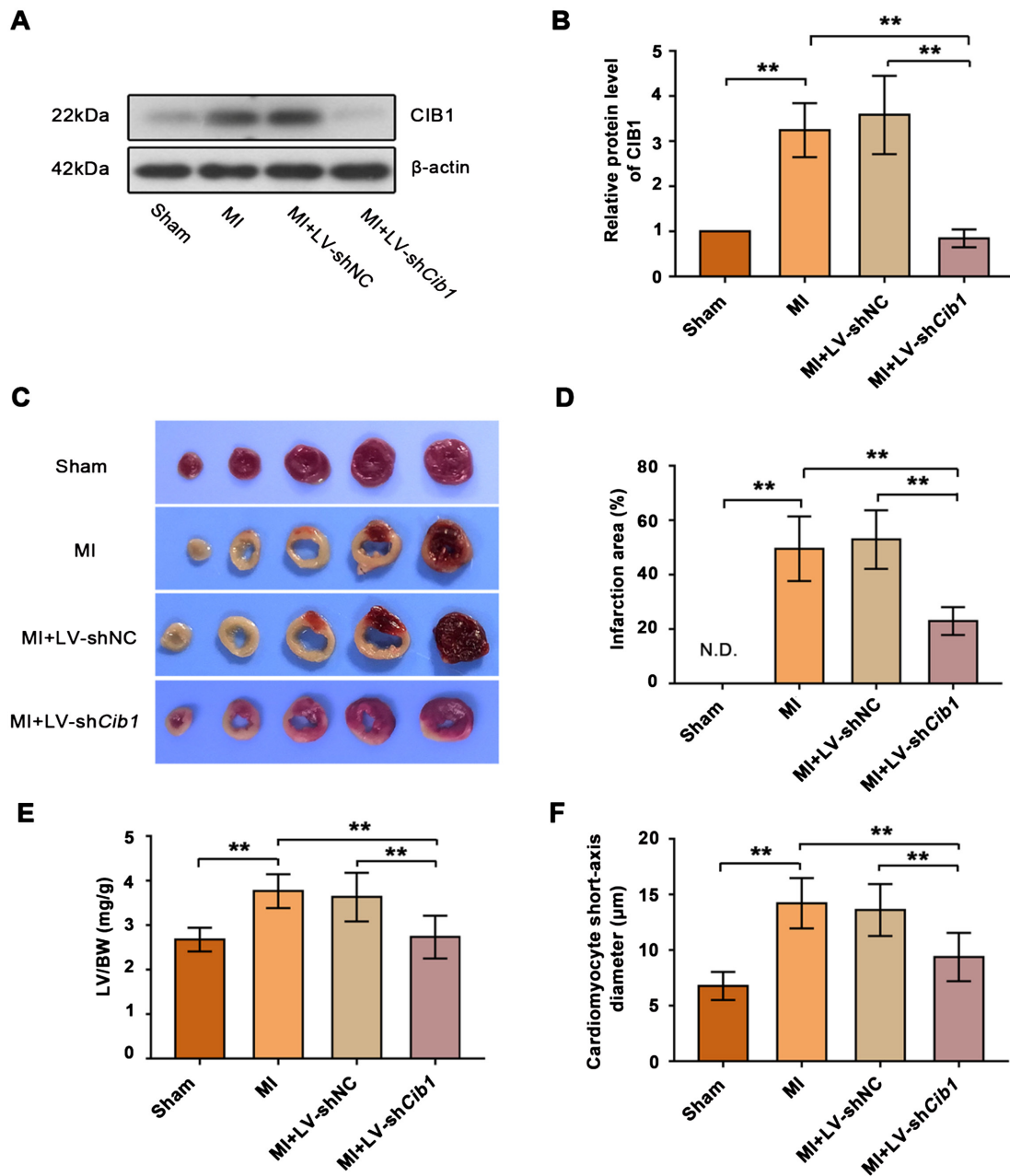


Fig. 3. CIB1 silencing relieves MI-induced myocardial damage and improves cardiac dysfunction. A–B. The images (A) and quantification (B) of CIB1 expression in the penumbra of the ischemic heart of the mice infected with *Cib1* RNA-interfering lentivirus detected with western blot. C–D. Representative images (C) and quantification (D) of heart infarct size detected with tetrazolium chloride (TTC) staining at 4 weeks post-MI. Normal tissue area (red) and infarcted tissue area (white) were measured, and the ratio of infarcted tissue area to the entire area was calculated. N.D.: not detected. E. The left ventricle-to-body weight ratio (LV/BW) of mice at 4 weeks post-MI. F. Cardiomyocyte short axis diameter measured in hematoxylin and eosin stained heart tissue sections at 4 weeks post-MI. Data are expressed as the mean \pm SD ($n=6/\text{group}$). $**P<0.01$.

suggesting that CIB1 downregulation represses activation of myofibroblasts induced by MI. Furthermore, the transcriptional levels of genes encoding vimentin (*Vim*), collagen I (*Col1a1*), and collagen III (*Col3a1*) were detected by real-time PCR. The expressions of these genes in the penumbra of the ischemic heart were also strongly induced by MI but repressed by CIB1 silencing (Figs. 4E–G). These findings demonstrate that the downregula-

tion of CIB1 mitigates MI-induced myocardial fibrosis by inhibiting the expressions of proteins involved in collagen production in mice.

The downregulation of CIB1 restrains Ang II-induced CFs transformation and collagen production *in vitro*

The CFs isolated from mice hearts were used to con-

Table 2. Cardiac function indexes in mice determined by Echo

Group	LVEDd (mm)	LVESd (mm)	FS (%)	EF (%)
Sham	2.267 ± 0.383	1.417 ± 0.2563	37.47 ± 4.306	67.43 ± 5.948
MI	4.017 ± 0.3971**	3.15 ± 0.2811**	21.47 ± 2.273**	46.95 ± 4.728**
MI+LV-shNC	4.233 ± 0.377	3.367 ± 0.2944	20.4 ± 3.718	44.65 ± 6.215
MI+LV-sh <i>Cib1</i>	2.983 ± 0.371 ^{###}	1.933 ± 0.1506 ^{###}	34.53 ± 7.736 ^{###}	64.28 ± 7.951 ^{###}

The FS and EF are significantly lower in MI group than those in sham group, while the LVEDd and LVESd are overtly higher in MI group than those in sham group, which are improved after CIB1 knockdown. ** $P < 0.01$ vs. sham group, ^{###} $P < 0.01$ vs. MI+LV-shNC group.

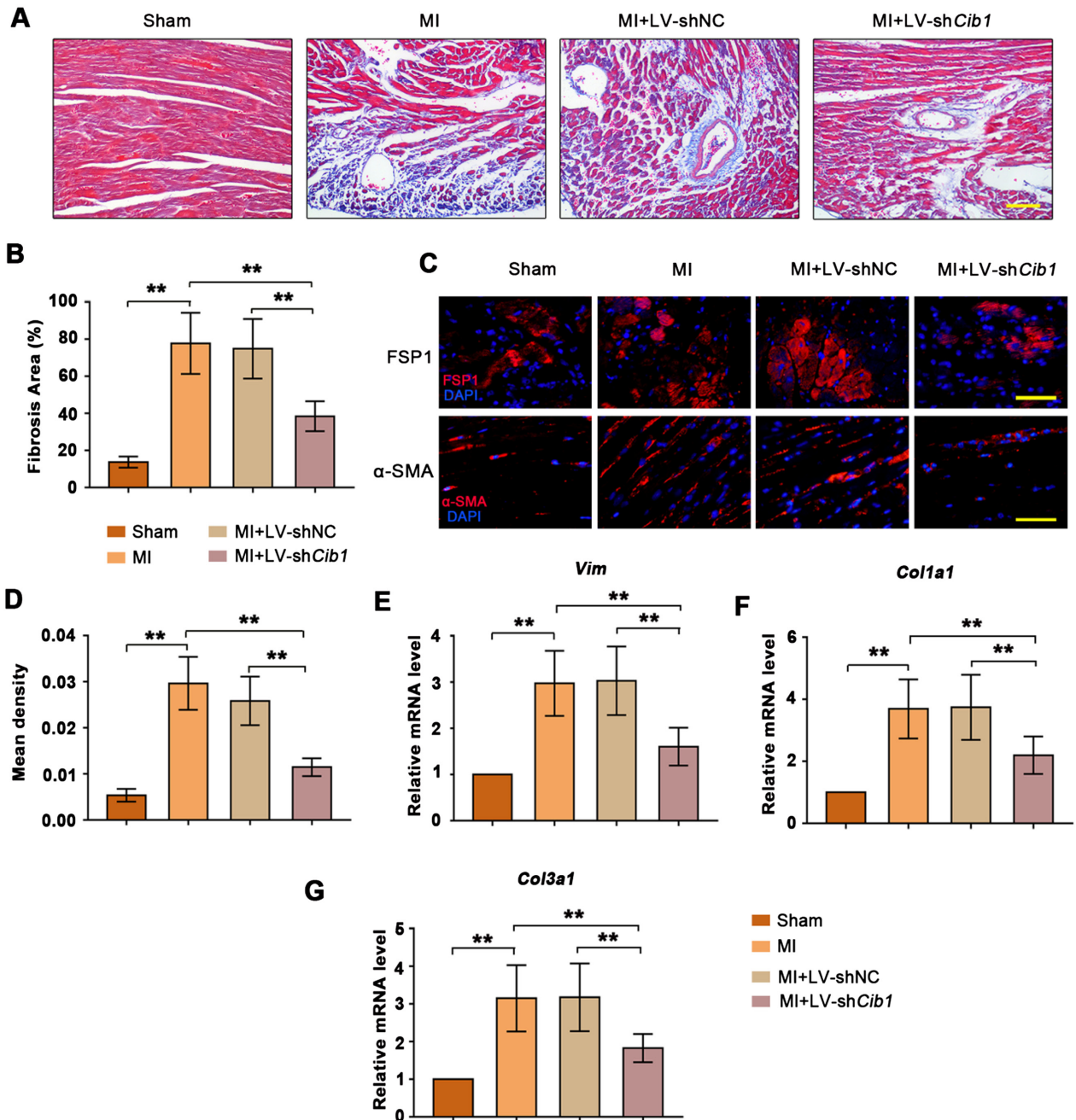


Fig. 4. CIB1 knockdown alleviates myocardial fibrosis caused by MI in mice. A. Masson's trichrome staining of heart slides at 4 weeks post-MI. The collagen fibers stained blue and the cell cytoplasm stained red. Magnification: 200×. Scale bar=100 μm. B. Percentage of the fibrotic area in Masson's trichrome staining. C. The representative images of FSP1 and α-SMA expression in the penumbra of ischemic heart in immunofluorescence staining. Magnification: 400×. Scale bar=50 μm. D. Quantification of α-SMA expression in the penumbra of ischemic heart at 4 weeks after MI modeling. E–G. The mRNA level of *Vim* (E), *Col1a1* (F), and *Col3a1* (G) in the penumbra of the ischemic heart measured with real-time PCR. Data are expressed as the mean ± SD (n=6/group). ** $P < 0.01$.

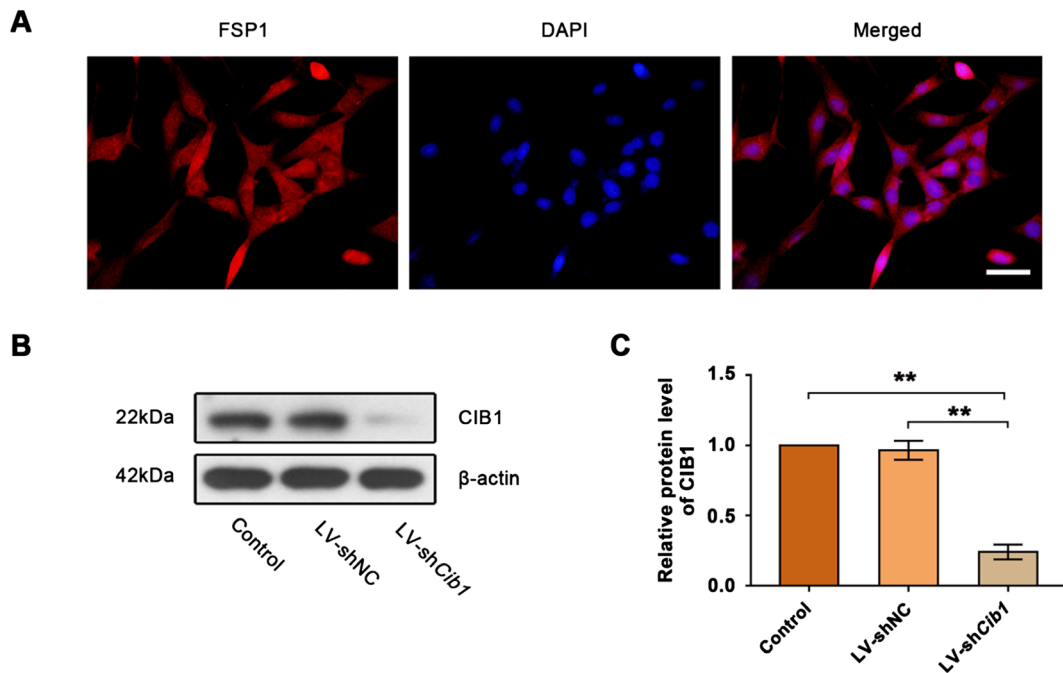


Fig. 5. Identification of cardiac fibroblasts (CFs) and CIB1 expression in the CFs. A. Immunofluorescence staining of FSP1 for the identification of cardiac fibroblasts (CFs). Magnification: 400 \times . Scale bar=50 μ m. B–C. Representative images (B) and quantification (C) of CIB1 protein expression in the CFs infected with *Cib1* RNA-interfering lentivirus. Data are expressed as the mean \pm SD (n=3/group). ** P <0.01.

firm the effects of CIB1 on myocardial fibrosis *in vitro*. FSP1 is a marker for the identification of CFs. Immunofluorescence staining of FSP1 showed that CFs were isolated from mice hearts successfully, and these cells could be used for modeling *in vitro* (Fig. 5A). The analysis of CIB1 protein level showed that the CFs infected with lentivirus expressing shRNA targeting *Cib1* exhibited a lower CIB1 protein level compared with normal cells (Figs. 5B and C). Ang II was used to induce cellular fibrosis *in vitro*, and the effects of CIB1 knockdown on CFs fibrosis were investigated (Fig. 6). The expression of α -SMA detected by IF was enhanced by Ang II and weakened in Ang II-treated cells when CIB1 was knocked down (Figs. 7A and B). Likewise, the mRNA levels of *Vim*, *Coll1a1*, and *Col3a1* were also analyzed in cells. Similar to the results in mice hearts, the silencing of CIB1 also downregulated the expressions of these genes in Ang II-treated CFs *in vitro* (Figs. 7C–E). These results indicate that the downregulation of CIB1 restrains Ang II-induced cardiac fibroblasts transformation and collagen production.

CIB1 depletion represses the PI3K/Akt signaling pathway activated by Ang II to prevent cellular fibrosis *in vitro*

To investigate the regulation of CIB1 to the PI3K/Akt signaling pathway, we analyzed the protein levels of phosphorylated p85 subunit of PI3K (p-PI3K-p85), total

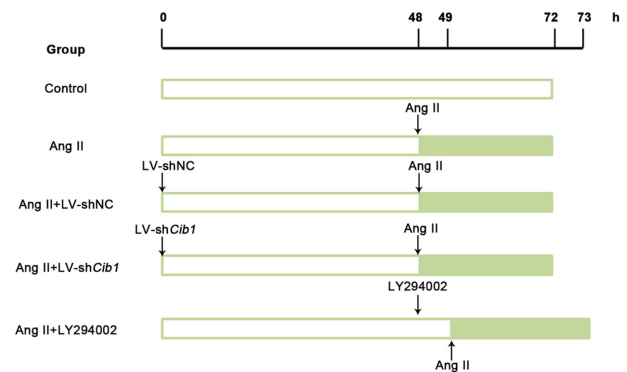


Fig. 6. The diagram of the investigation of CIB1 function in angiotensin II (Ang-II)-induced cardiac fibroblasts fibrosis *in vitro*. To analyze the effects of CIB1 knockdown on CFs fibrosis, the CFs were infected with *Cib1* RNA-interfering lentivirus (LV-sh*Cib1*) or its negative control lentivirus (LV-shNC) followed by Ang-II treatment at 48 h post-injection. For the signaling pathway analysis, the CFs were subjected to an inhibitor of the PI3K/Akt pathway, LY294002, before Ang-II treatment.

p85 subunit of PI3K (PI3K-p85), phosphorylated Akt (p-Akt), and total Akt in CFs. Notably, Ang II elevated the level of p-PI3K-p85 in CFs, and CIB1 knockdown in Ang II-treated cells repressed the phosphorylation of PI3K-p85. In contrast, the total level of PI3K-p85 between the different groups displays no significant difference (Figs. 8A and B). Also, CIB1 silencing reduced the level of p-Akt which was increased by Ang II in cells

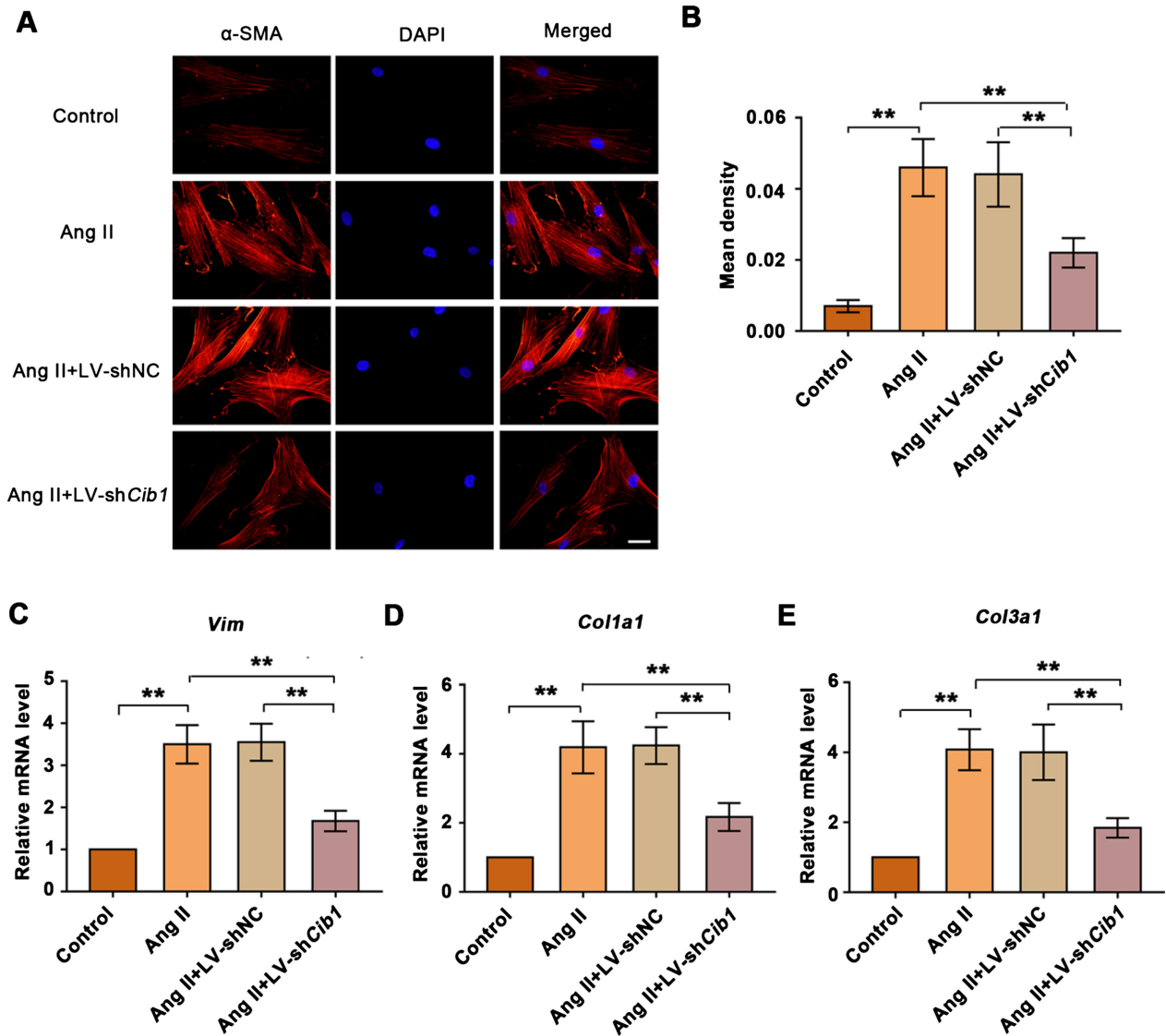


Fig. 7. Down-regulation of CIB1 restrains angiotensin II (Ang II)-induced cardiac fibroblasts (CFs) transformation and collagen production *in vitro*. A–B. The images (A) and quantification (B) of immunofluorescent staining for α -SMA expression in Ang II-treated CFs. Magnification: 400 \times . Scale bar=50 μ m. C–E. The mRNA level of *Vim* (C), *Col1a1* (D), and *Col3a1* (E) in the Ang II-treated CFs measured with real-time PCR. Data are expressed as the mean \pm SD (n=3/group). ** P <0.01.

without altering the total Akt level (Figs. 8C and D). Therefore, the downregulation of CIB1 inhibited the activation of the PI3K/Akt signaling pathway in CFs induced by Ang II. To confirm that the effects of CIB1 on myocardial fibrosis were mediated by the PI3K/Akt signaling pathway, LY294002, a PI3K/Akt pathway inhibitor, was added to pre-treat CFs before Ang II treatment (Fig. 6). The protein level of α -SMA and collagen I detected by western blot showed that the inhibition of the PI3K/Akt signaling pathway suppressed the expressions of α -SMA and collagen I and CIB1 knockdown exert a similar effect on these two protein expressions with LY294002 (Figs. 8E and F). Further, CIB1 knockdown may play an anti-fibrosis role by repressing the PI3K/Akt signaling pathway in CFs.

Discussion

CIB1 is upregulated in the urine of patients with both acute and chronic ischemic heart failure, the right atrial myocardium of patients with atrial fibrillation, and the peripheral blood mononuclear cells of the patients with the acute coronary syndrome [14–16]. In this study, we proved that CIB1 was also upregulated in the heart tissues of MI mice, suggesting that MI strongly induced CIB1 expression. There has been little research about the function of CIB1 in heart diseases, especially in MI. Heart failure following MI occurs with ventricular dilatation, scar thinning, and activation of interstitial fibrosis [27, 28]. Fluid overload, myocardial hypertrophy, and ongoing cardiomyocyte death lead to further deteriora-

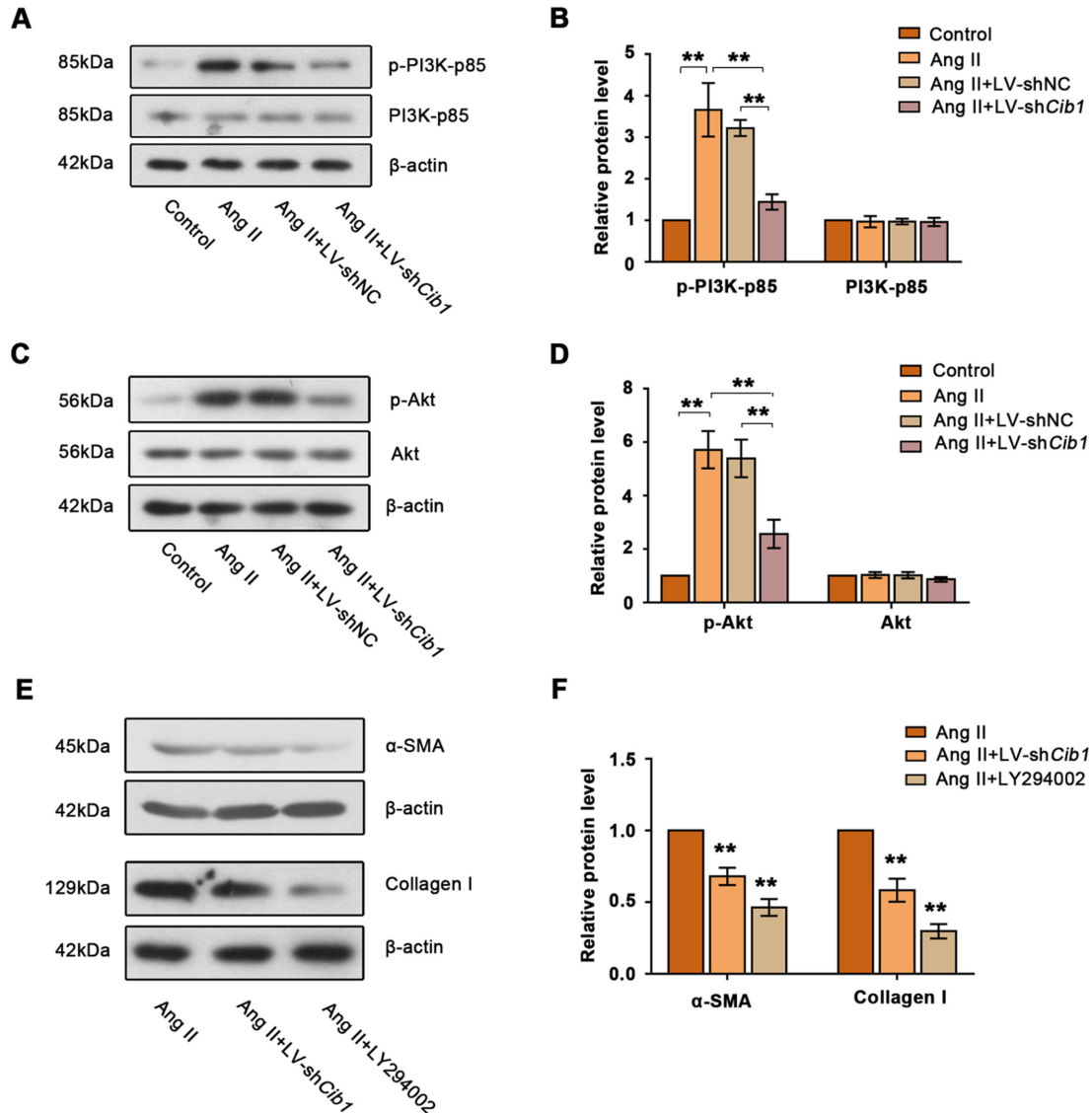


Fig. 8. CIB1 depletion represses the PI3K/Akt signaling pathway activated by Ang II to prevent cardiac fibroblasts (CFs) fibrosis. A–B. Representative images (A) and quantification (B) of phosphorylated PI3K-p85 (p-PI3K-p85) and total PI3K-p85 protein expression in Ang II-treated CFs, analyzed by western blot. C–D. Representative images (C) and quantification (D) of phosphorylated Akt (p-Akt) and total Akt protein expression in Ang II-treated CFs. E–F. Representative images (E) and quantification (F) of α -SMA and Collagen I levels in Ang II-treated CFs when CIB1 was knocked down or LY294002 (an inhibitor of the PI3K/Akt pathway) was added. Data are expressed as the mean \pm SD (n=3/group). ** P <0.01 vs. Ang II.

tion in ventricular function [29, 30]. Therefore, we analyzed cardiac dysfunction and fibrosis in MI after CIB1 silencing. Our results showed that CIB1 silencing improved cardiac function impaired by MI, reduced the infarct size in the heart, and alleviated cardiac hypertrophy induced by MI. Similarly, Heineke's study shows that *Cib1*-deleted mice exhibit a marked alleviation in myocardial hypertrophy, and overexpression of CIB1 augments myocardial hypertrophy [17]. CIB1, as a hypertrophic activator of the calcineurin-nuclear factor of activated T cells (NFAT) signaling in maladaptive programming of cardiac growth, is necessary for cardiac hypertrophy [17, 31, 32]. Moreover, fibrosis is the exces-

sive accumulation of collagen and other extracellular matrix (ECM) components which enhances ventricular stiffness and causes abnormal diastolic relaxation and filling, triggering cardiac dysfunction [33]. The results of myocardial fibrosis both *in vivo* and *in vitro* indicated that CIB1 downregulation repressed the expressions of related proteins, including α -SMA, vimentin, Collagen I, and Collagen III, resulting in the inhibition of collagen production and myocardial fibrosis. Likewise, during pressure overload, the inhibition of CIB1 represses cardiac hypertrophy and fibrosis and initially improved cardiac function [17, 34]. In this research, we demonstrated that CIB1 contributed to the development of MI

and its depletion played an anti-fibrotic role and preserved cardiac function in MI.

According to the previous studies, the PI3K/Akt signaling pathway is involved in fibrosis after MI, but the effect of this pathway in myocardial fibrosis is still controversial. On the one hand, the activation of the PI3K/Akt pathway attenuates fibrosis in MI. For instance, astragaloside IV and grape seed proanthocyanidin extract both exert cardioprotection, including attenuating fibrosis after MI by activating the PI3K/AKT pathway [35, 36]. Conversely, it has been reported that the activation of the PI3K/Akt pathway also promotes myocardial fibrosis after MI. Apelin-13 alleviated cardiac fibrosis *via* inhibiting the PI3K/Akt pathway in MI-induced heart failure [22]. We speculate that different molecules or drugs may target different downstream genes or proteins in the PI3K/Akt pathway, resulting in the contrary effects of the PI3K/Akt pathway on fibrosis. In our study, deactivation of this pathway repressed fibrosis and reducing collagen production in CFs. In addition to fibrosis, the deletion of genes encoding Akt1 caused reduced cardiac hypertrophy and the development of heart failure in mice [37]. However, the role of CIB1 in the PI3K/Akt pathway is limited. In MDA-MB-468 breast cancer and SK-N-SH neuroblastoma cells, RNAi knockdown of *Cib1* significantly reduced the activity of Akt, a vital component of the PI3K/Akt pathway [38]. In the present study, we demonstrated that the PI3K/Akt pathway was activated by MI *in vivo* and *in vitro*, and CIB1 silencing repressed the activation of this pathway. Consistent with the previous study, the deactivation of the PI3K/Akt pathway caused by CIB1 knockdown attenuates myocardial fibrosis and cardiac dysfunction induced by MI, indicating that CIB1 downregulation may exert a protective effect in MI *via* inhibiting the PI3K/Akt signaling pathway. We have confirmed the role of CIB1 in the activation of the PI3K/Akt pathway after MI in this study. Still, the following mechanism and the relationship between the PI3K/Akt pathway and myocardial fibrosis remain to be investigated more deeply.

CIB1 was first discovered as a binding partner of the α IIb integrin, but the binding partner of CIB1 in cardiac fibroblasts was unknown in this study. Besides α IIb integrin, CIB1 is reported to interact with other integrins such as integrin α 2, α 3, α 4, and α 5 [8]. Some integrins are involved in the activation of the PI3K/Akt pathway. For instance, the blockade of α 2 β 1 weakens PI3K/Akt signal in human colorectal cancer cell line HCT-116 and mouse colorectal cancer cell line CT-26 [39]. Integrin α 2 and α 5 could activate PI3K/Akt signaling pathway [40, 41]. Activation of the integrin α 5 β 1/PI3K/Akt signaling pathway induces hepatic stellate cell activation,

proliferation, and migration and leads to liver fibrosis [42]. Based on the previous research and current study findings, we speculate that CIB1 knockdown may inhibit the PI3K/Akt signaling pathway by interacting with integrin α 2, α 5, or other integrins, thus alleviating MI-induced cardiac fibrosis. However, whether or how CIB1 regulates MI-induced cardiac fibrosis via these integrins needs further exploration.

Furthermore, the inactivation of the PI3K/Akt signaling pathway mediated by CIB1 knockdown is necessary for the abnormal translocation and accumulation of glyceraldehyde 3-phosphate dehydrogenase in the nucleus which can lead to subsequent nonapoptotic and GAPDH-dependent cell death in cancer [38]. Also, CIB1 mitigated apoptotic cell death of dopaminergic cells [43]. The overexpression of CIB1 in HeLa cells causes apoptosis [44]. Thereby, CIB1 may play contradictory roles in the apoptosis of diverse cell types under different environments. According to these findings, we hypothesize that CIB1 functions not only in myocardial fibrosis but also in cell death or apoptosis in the heart after MI by regulating the PI3K/Akt signaling pathway, which was not explored in the current study but will be confirmed in the future.

In summary, CIB1 is upregulated in MI, which upregulates the expressions of proteins in collagen production, including vimentin, Collagen I, and Collagen III through activating the PI3K/Akt signaling pathway and then induces myocardial fibrosis, resulting in cardiac dysfunction after MI (Fig. 9). Thus, CIB1 knockdown

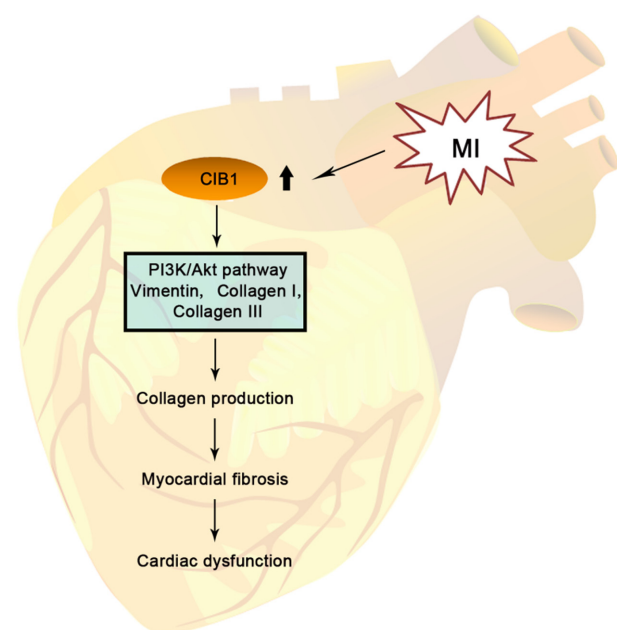


Fig. 9. The diagram of the potential mechanism of CIB1 in myocardial infarction (MI).

can attenuate these myocardial damages caused by MI, which may be a potential candidate for targeted therapies in cardiovascular disease, including MI.

Ethics Approval

The animal experiments were approved by the ethics committee of the First Affiliated Hospital of Anhui Medical University (No.LLSC20201117).

Conflict of Interests

The authors declare that there is no conflict of interest regarding the publication of this paper.

Author Contributions

All persons who meet authorship criteria are listed as authors. Guangquan Hu and Jiehua Li contributed to the conception of the work. Xiaojie Ding and Feng Gao performed the experiments. Guangquan Hu and Xiaojie Ding analyzed the data. Guangquan Hu drafted the manuscript. Jiehua Li revised the manuscript.

Data Availability Statement

The data that support the findings of this study are available from the corresponding author upon reasonable request.

Acknowledgments

This study was supported by the Anhui Province Key Research and Development Plan (No.201904a07020041).

References

1. Thygesen K, Alpert JS, Jaffe AS, Chaitman BR, Bax JJ, Morrow DA, et al. Executive Group on behalf of the Joint European Society of Cardiology (ESC)/American College of Cardiology (ACC)/American Heart Association (AHA)/World Heart Federation (WHF) Task Force for the Universal Definition of Myocardial Infarction. Fourth Universal Definition of Myocardial Infarction (2018). *J Am Coll Cardiol.* 2018; 72: 2231–2264. [Medline] [CrossRef]
2. Sahoo S, Losordo DW. Exosomes and cardiac repair after myocardial infarction. *Circ Res.* 2014; 114: 333–344. [Medline] [CrossRef]
3. Boon RA, Dimmeler S. MicroRNAs in myocardial infarction. *Nat Rev Cardiol.* 2015; 12: 135–142. [Medline] [CrossRef]
4. Barnett R. Acute myocardial infarction. *Lancet.* 2019; 393: 2580. [Medline] [CrossRef]
5. Cahill TJ, Choudhury RP, Riley PR. Heart regeneration and repair after myocardial infarction: translational opportunities for novel therapeutics. *Nat Rev Drug Discov.* 2017; 16: 699–717. [Medline] [CrossRef]
6. Anavekar NS, McMurray JJ, Velazquez EJ, Solomon SD, Kober L, Rouleau JL, et al. Relation between renal dysfunction and cardiovascular outcomes after myocardial infarction. *N Engl J Med.* 2004; 351: 1285–1295. [Medline] [CrossRef]
7. Naik UP, Patel PM, Parise LV. Identification of a novel calcium-binding protein that interacts with the integrin alphaIIb cytoplasmic domain. *J Biol Chem.* 1997; 272: 4651–4654. [Medline] [CrossRef]
8. Leisner TM, Freeman TC, Black JL, Parise LV. CIB1: a small protein with big ambitions. *FASEB J.* 2016; 30: 2640–2650. [Medline] [CrossRef]
9. Zhu W, Gliddon BL, Jarman KE, Moretti PAB, Tin T, Parise LV, et al. CIB1 contributes to oncogenic signalling by Ras via modulating the subcellular localisation of sphingosine kinase 1. *Oncogene.* 2017; 36: 2619–2627. [Medline] [CrossRef]
10. Naik MU, Pham NT, Beebe K, Dai W, Naik UP. Calcium-dependent inhibition of polo-like kinase 3 activity by CIB1 in breast cancer cells. *Int J Cancer.* 2011; 128: 587–596. [Medline] [CrossRef]
11. Black JL, Harrell JC, Leisner TM, Fellmeth MJ, George SD, Reinhold D, et al. CIB1 depletion impairs cell survival and tumor growth in triple-negative breast cancer. *Breast Cancer Res Treat.* 2015; 152: 337–346. [Medline] [CrossRef]
12. Saito T, Seki N, Hattori A, Hayashi A, Abe M, Araki R, et al. Structure, expression profile, and chromosomal location of a mouse gene homologous to human DNA-PKcs interacting protein (KIP) gene. *Mamm Genome.* 1999; 10: 315–317. [Medline] [CrossRef]
13. Shock DD, Naik UP, Brittain JE, Alahari SK, Sondek J, Parise LV. Calcium-dependent properties of CIB binding to the integrin alphaIIb cytoplasmic domain and translocation to the platelet cytoskeleton. *Biochem J.* 1999; 342: 729–735. [Medline] [CrossRef]
14. Zhang L, Tang F, Cai LP, Wang HL, Wang Z. Research on the correlation of urine calcium integrin binding protein-1 and pro-BNP with ischemic heart failure. *Eur Rev Med Pharmacol Sci.* 2017; 21: 4181–4185. [Medline]
15. Zhao F, Zhang S, Chen L, Wu Y, Qin J, Shao Y, et al. Calcium- and integrin-binding protein-1 and calcineurin are upregulated in the right atrial myocardium of patients with atrial fibrillation. *Europace.* 2012; 14: 1726–1733. [Medline] [CrossRef]
16. Dabek J, Ligus J, Szota J. Oligonucleotide microarray and QRT-PCR study of adhesion protein gene expression in acute coronary syndrome patients. *Inflammation.* 2010; 33: 398–407. [Medline] [CrossRef]
17. Heineke J, Auger-Messier M, Correll RN, Xu J, Benard MJ, Yuan W, et al. CIB1 is a regulator of pathological cardiac hypertrophy. *Nat Med.* 2010; 16: 872–879. [Medline] [CrossRef]
18. Reichert K, Colantuono B, McCormack I, Rodrigues F, Pavlov V, Abid MR. Murine Left Anterior Descending (LAD) Coronary Artery Ligation: An Improved and Simplified Model for Myocardial Infarction. *J Vis Exp.* 2017; (122): 55353. [Medline]
19. Chen L, Wang GY, Dong JH, Cheng XJ. MicroRNA-132 improves myocardial remodeling after myocardial infarction. *Eur Rev Med Pharmacol Sci.* 2019; 23: 6299–6306. [Medline]
20. Marino A, Zhang Y, Rubinelli L, Riemma MA, Ip JE, Di Lorenzo A. Pressure overload leads to coronary plaque formation, progression, and myocardial events in ApoE^{-/-} mice. *JCI Insight.* 2019; 4: e128220. [Medline] [CrossRef]
21. Ishikawa K, Aguero J, Tilemann L, Ladage D, Hammoudi N, Kawase Y, et al. Characterizing preclinical models of ischemic heart failure: differences between LAD and LCx infarctions. *Am J Physiol Heart Circ Physiol.* 2014; 307: H1478–H1486. [Medline] [CrossRef]
22. Zhong S, Guo H, Wang H, Xing D, Lu T, Yang J, et al. Apelin-13 alleviated cardiac fibrosis via inhibiting the PI3K/Akt pathway to attenuate oxidative stress in rats with myocardial infarction-induced heart failure. *Biosci Rep.* 2020; 40: BSR20200040. [Medline] [CrossRef]

23. Zhang K, He X, Zhou Y, Gao L, Qi Z, Chen J, et al. Atorvastatin Ameliorates Radiation-Induced Cardiac Fibrosis in Rats. *Radiat Res.* 2015; 184: 611–620. [[Medline](#)] [[CrossRef](#)]
24. Dineva IK, Zaharieva MM, Konstantinov SM, Eibl H, Berger MR. Erufosine suppresses breast cancer in vitro and in vivo for its activity on PI3K, c-Raf and Akt proteins. *J Cancer Res Clin Oncol.* 2012; 138: 1909–1917. [[Medline](#)] [[CrossRef](#)]
25. Iyer RP, de Castro Brás LE, Cannon PL, Ma Y, DeLeon-Pennell KY, Jung M, et al. Defining the sham environment for post-myocardial infarction studies in mice. *Am J Physiol Heart Circ Physiol.* 2016; 311: H822–H836. [[Medline](#)] [[CrossRef](#)]
26. Yang W, Wu Z, Yang K, Han Y, Chen Y, Zhao W, et al. BMI1 promotes cardiac fibrosis in ischemia-induced heart failure via the PTEN-PI3K/Akt-mTOR signaling pathway. *Am J Physiol Heart Circ Physiol.* 2019; 316: H61–H69. [[Medline](#)] [[CrossRef](#)]
27. Pfeffer MA, Braunwald E. Ventricular remodeling after myocardial infarction. Experimental observations and clinical implications. *Circulation.* 1990; 81: 1161–1172. [[Medline](#)] [[CrossRef](#)]
28. Sutton MG, Sharpe N. Left ventricular remodeling after myocardial infarction: pathophysiology and therapy. *Circulation.* 2000; 101: 2981–2988. [[Medline](#)] [[CrossRef](#)]
29. Narula J, Haider N, Arbustini E, Chandrashekar Y. Mechanisms of disease: apoptosis in heart failure—seeing hope in death. *Nat Clin Pract Cardiovasc Med.* 2006; 3: 681–688. [[Medline](#)] [[CrossRef](#)]
30. Packer M. The neurohormonal hypothesis: a theory to explain the mechanism of disease progression in heart failure. *J Am Coll Cardiol.* 1992; 20: 248–254. [[Medline](#)] [[CrossRef](#)]
31. Frost RJ, Olson EN. Separating the good and evil of cardiac growth by CIB1 and calcineurin. *Cell Metab.* 2010; 12: 205–206. [[Medline](#)] [[CrossRef](#)]
32. Bourajaj M, Armand AS, da Costa Martins PA, Weijts B, van der Nagel R, Heeneman S, et al. NFATc2 is a necessary mediator of calcineurin-dependent cardiac hypertrophy and heart failure. *J Biol Chem.* 2008; 283: 22295–22303. [[Medline](#)] [[CrossRef](#)]
33. Yang J, Savvatis K, Kang JS, Fan P, Zhong H, Schwartz K, et al. Targeting LOXL2 for cardiac interstitial fibrosis and heart failure treatment. *Nat Commun.* 2016; 7: 13710. [[Medline](#)] [[CrossRef](#)]
34. Grund A, Szaroszyk M, Döppner JK, Malek Mohammadi M, Kattih B, Korf-Klingebiel M, et al. A gene therapeutic approach to inhibit calcium and integrin binding protein 1 ameliorates maladaptive remodelling in pressure overload. *Cardiovasc Res.* 2019; 115: 71–82. [[Medline](#)] [[CrossRef](#)]
35. Cheng S, Zhang X, Feng Q, Chen J, Shen L, Yu P, et al. Astragaloside IV exerts angiogenesis and cardioprotection after myocardial infarction via regulating PTEN/PI3K/Akt signaling pathway. *Life Sci.* 2019; 227: 82–93. [[Medline](#)] [[CrossRef](#)]
36. Ruan Y, Jin Q, Zeng J, Ren F, Xie Z, Ji K, et al. Grape Seed Proanthocyanidin Extract Ameliorates Cardiac Remodelling After Myocardial Infarction Through PI3K/AKT Pathway in Mice. *Front Pharmacol.* 2020; 11: 585984. [[Medline](#)] [[CrossRef](#)]
37. DeBosch B, Treskov I, Lupu TS, Weinheimer C, Kovacs A, Courtois M, et al. Akt1 is required for physiological cardiac growth. *Circulation.* 2006; 113: 2097–2104. [[Medline](#)] [[CrossRef](#)]
38. Leisner TM, Moran C, Holly SP, Parise LV. CIB1 prevents nuclear GAPDH accumulation and non-apoptotic tumor cell death via AKT and ERK signaling. *Oncogene.* 2013; 32: 4017–4027. [[Medline](#)] [[CrossRef](#)]
39. Wu X, Cai J, Zuo Z, Li J. Collagen facilitates the colorectal cancer stemness and metastasis through an integrin/PI3K/AKT/Snail signaling pathway. *Biomed Pharmacother.* 2019; 114: 108708. [[Medline](#)] [[CrossRef](#)]
40. Zheng H, Tian Y, Gao Q, Yu Y, Xia X, Feng Z, et al. Hierarchical Micro-Nano Topography Promotes Cell Adhesion and Osteogenic Differentiation via Integrin α 2-PI3K-AKT Signaling Axis. *Front Bioeng Biotechnol.* 2020; 8: 463. [[Medline](#)] [[CrossRef](#)]
41. Hou S, Jin W, Xiao W, Deng B, Wu D, Zhi J, et al. Integrin α 5 promotes migration and cisplatin resistance in esophageal squamous cell carcinoma cells. *Am J Cancer Res.* 2019; 9: 2774–2788. [[Medline](#)]
42. Du Z, Lin Z, Wang Z, Liu D, Tian D, Xia L. SPOCK1 overexpression induced by platelet-derived growth factor-BB promotes hepatic stellate cell activation and liver fibrosis through the integrin α 5 β 1/PI3K/Akt signaling pathway. *Lab Invest.* 2020; 100: 1042–1056. [[Medline](#)] [[CrossRef](#)]
43. Yoon KW, Cho JH, Lee JK, Kang YH, Chae JS, Kim YM, et al. CIB1 functions as a Ca(2+)-sensitive modulator of stress-induced signaling by targeting ASK1. *Proc Natl Acad Sci USA.* 2009; 106: 17389–17394. [[Medline](#)] [[CrossRef](#)]
44. Stabler SM, Ostrowski LL, Janicki SM, Monteiro MJ. A myristoylated calcium-binding protein that preferentially interacts with the Alzheimer's disease presenilin 2 protein. *J Cell Biol.* 1999; 145: 1277–1292. [[Medline](#)] [[CrossRef](#)]